

5 Applied studies: Radionuclide behavior in the multi-barrier system

Long-term safety of a deep geological repository for nuclear waste depends on a multi-barrier system which consists of technical and geo-technical barriers such as the waste form, the canister, backfilling and sealing of the mined openings as well as on the natural barrier function of the host rock. At KIT-INE, a series of applied studies on subsystems of various multi-barrier systems are performed, which cover a variety of components with specific characteristics and properties. Investigations presented in the first sub-chapter cover the experimental quantification of radionuclide release from spent nuclear fuel under strongly reducing conditions and the determination of the chemical form of C-14 present in irradiated steel sampled from a fuel rod segment. In the following, we describe activities on preservation of know-how with respect to results of R&D in the field of radioactive waste management performed at the former Research Centre Karlsruhe / Kernforschungszentrum Karlsruhe. The third sub-chapter deals with formation of colloids and impact of colloids on radionuclide migration in various technical, geo-technical and geological barriers of a multi-barrier system. We report on results of experimental studies on long-term Lu incorporation into iron-(hydr)oxides phases, characterization of natural organic matter and interaction of natural organic colloids with radionuclides, erosion of compacted bentonite erosion and formation of bentonitic colloids, bentonitic colloids radionuclide sorption, and interactions of synthetic colloids with mineral surfaces. In addition to these experimental studies, modelling studies on coupled processes in the near-field of geological repositories are conducted. In the final sub-chapter, modelling studies on coupled processes at the concrete / clay interface with respect to a repository in an argillaceous host rock and the effect of fracture geometry on bentonite erosion with respect to a repository in a crystalline host rock are described.

5.1 Highly radioactive waste forms

E. González-Robles, M. Herm, N. Müller, M. Böttle, E. Bohnert, B. Kienzler, V. Metz

In collaboration with:

R. Dagan^a, D. Papaioannou^b

^a Karlsruhe Institute of Technology, Institute for Neutron Physics and Reactor Technology, Karlsruhe, Germany; ^b European Commission, Joint Research Centre, Karlsruhe, Germany

Matrix dissolution of spent nuclear fuel under H₂ overpressure in bicarbonate water

Introduction

In case of container failure in a deep geological repository for spent nuclear fuel (SNF), intruding water possibly gets into contact with the waste. Besides anaerobic corrosion of the container material and consecutive production of hydrogen, radionuclides will be released into the groundwater [1,2].

Initially a fast radionuclide release is expected to occur, which will include the release of fission gases and volatile radionuclides segregated at the gap between fuel and cladding, at fuel fractures and at grain boundaries. Simultaneously to the fast leaching of the so-called instant release fraction, a relatively slow dissolution of the fuel matrix will begin, resulting in the release of matrix-bound radionuclides. The matrix dissolution is a long-term process, which will continue after the fast leaching processes will have been ceased.

Dissolution of the fuel matrix will be affected both by the presence of molecular hydrogen and by water radiolysis. The later will result in the production of oxidizing radiolysis products (e.g. OH radicals and H₂O₂) in the micrometer scale vicinity of the fuel surface that might enhance the matrix dissolution,

even if reducing conditions are expected to prevail within the near-field of the deep geological repository. The present study focuses on the impact of H₂ overpressure on the release of uranium and other matrix-bound radionuclides, in particular actinides. Therefore, the dissolution behavior of an irradiated UO₂ fuel with an average burn-up of 50.4 MWd/kg_{HM} was studied under deep geological repository conditions with a simulated near neutral pH groundwater and H₂ overpressure.

Spent nuclear fuel samples

The studied SNF samples were taken from the SBS1108 N0204 fuel rod segment, which was irradiated in the pressurized water reactor of the Gösgen nuclear power plant in Switzerland.

The irradiation was carried out in four cycles for a period of time of 1226 days with an average linear power rate of 260 W/cm and achieving an average burn-up of 50.4 GWd/t_{HM}. The fuel rod segment was discharged the 27th of May 1989 that implies a cooling time of 24 years before characterization and cutting of the segment.

Characteristic data of the studied SBS1108 N0204 fuel rod segment are given in [3,4]. Based on results of a puncturing test of the fuel rod segment, the fission gas release into the plenum of the segment was previously calculated to be 8.35% [4,5].

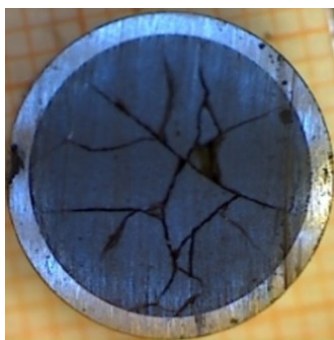


Fig. 1: Bottom side of the cladded pellet used in the first SNF dissolution experiment.



Fig. 2: Fragments obtained from the decladding of a pellet used in the second SNF dissolution experiment.

Sample preparation

Two cladded fuel pellets were cut from the fuel rod segment and were used in two leaching experiments. The complete sampling process is described elsewhere [4, 6].

The first leaching experiment was performed with a cladded pellet, whereas the second experiment was performed with SNF fragments. Therefore, the second pellet was decladded in order to get fragments and to separate the fuel from the Zircaloy (the cladding was not used during the leaching experiment).

Prior to the start of the experiments, both SNF samples were weighed. In the case of the cladded pellet, the length and diameter of the sample were measured too. The weight of the cladded pellet was (7.77 ± 0.01) g, the length (9.85 ± 0.01) mm with and external and internal diameter of (10.75 ± 0.01) and (9.35 ± 0.01) mm, respectively. The weight of the fuel without cladding was calculated to be (6.97 ± 0.01) g, taking into account the internal diameter) and the length of the fuel pellet. In case of the fragments, their total weight was (5.69 ± 0.01) g and the average size was determined to be 1 mm.

Images of the cladded pellet and the fragments used during the leaching experiments are given in figures 1 and 2.

Experimental set-up of leaching experiments

Both tests were conducted as static leaching experiments in 250 mL stainless steel Ti-lined VA autoclaves (Berghof Company, Eningen, Germany).

The composition of the bicarbonate leaching solution used in each of the experiments was as following: 19 mM NaCl + 1 mM NaHCO₃ with a pH of (8.9 ± 0.2) and $E_{h(vs\ SHE)}$ of (-116.3 ± 50) mV.

The leachant for the two experiments was prepared in a glove-box under Ar atmosphere. The experiments themselves were carried out in an Ar / H₂ atmosphere with a total pressure of (40 ± 1) bar, with a partial pressure of H₂ of (3.2 ± 0.1) bar, at room temperature.

In the case of the experiment with the cladded pellet, the sample was mounted in a Ti sample holder to ensure the contact of the top and bottom surfaces of the pellet with the solution, whereas the fragments were kept in a glass basket.

Once the samples were placed into the autoclaves, they were closed and flushed with Ar to avoid any possible presence of air.

Afterwards, a pre-leaching test with duration of 1 day was performed by filling each autoclave with (220 ± 1) mL of the bicarbonate leaching solution mentioned above. This pre-leaching step was performed in order to reduce the amount of Cs in solution and to remove any pre-oxidation layer potentially present at the surface of the SNF samples. After the pre-leaching, a gas sample was collected and the solution was completely purged. Then each autoclave was again replenished with (220 ± 1) mL of bicarbonate solution as described above.

Gaseous (50 ± 1) mL and liquid (15 ± 1) mL samples were taken at certain time steps. After the sampling, the gas volume of the autoclaves was purged with Ar, and the initial conditions (40 bar of Ar + H₂ mixture) were again established. The solution was not renewed after sampling, thus the remaining leachant volume was reduced at each sampling step.

From the liquid samples obtained during each campaign different aliquots were prepared to determine the amount of ²³⁷Np, ²³⁸U, ²³⁹Pu, ²⁴³Am and ²⁴⁴Cm as following: A (5.0 ± 0.1) mL aliquot was acidified and, subsequently, ammonium molybdate phosphate (AMP) was added to remove Cs by precipitation giving as a result a free Cs solution with a lower activity than the original one.

From this aliquot, (2.5 ± 0.1) mL were analyzed by means of Inductively Coupled Plasma Mass Spectrometry (ELAN 6100 Perkin Elmer Inc, Waltham, USA) to quantify ²³⁷Np, ²³⁸U, ²³⁹Pu, ²⁴³Am and ²⁴⁴Cm dissolved in solution.

The pH and Eh of the samples were measured at the end of the four experiments to avoid possible air intrusion that in the case of the Eh measurement would have given unrealistic values. The device and the procedure followed is the same as stated in [7].

At the end of each experiment the pH was (8.7 ± 0.5) and the $E_{h(vs\ SHE)}$ was (-518 ± 50) mV for the pellet and (-418 ± 50) mV for the fragments.

Results and Discussion

Aqueous concentrations of ²³⁷Np, ²³⁸U, ²³⁹Pu, ²⁴³Am and ²⁴⁴Cm in both SNF dissolution experiments are shown in figures 3 and 4.

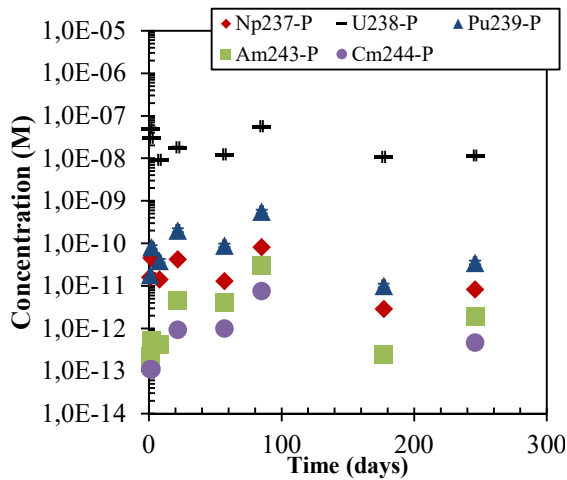


Fig. 3: Aqueous concentrations of ^{237}Np , ^{238}U , ^{239}Pu , ^{243}Am and ^{244}Cm as a function of time in the dissolution experiment performed with a cladded SNF pellet.

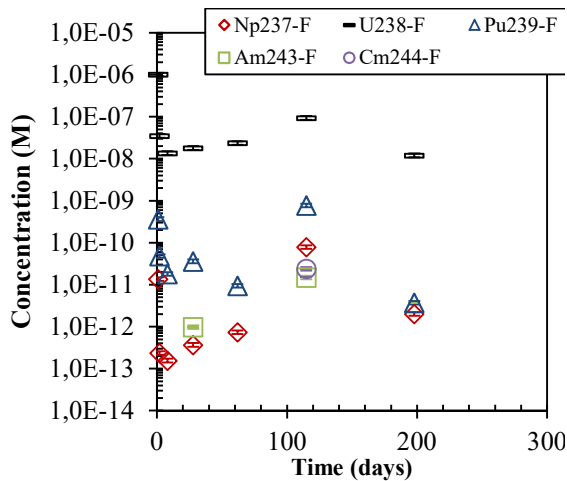


Fig. 4: Aqueous concentrations of ^{237}Np , ^{238}U , ^{239}Pu , ^{243}Am and ^{244}Cm as a function of time in the dissolution experiment performed with SNF fragments.

In order to interpret the measured radionuclide concentrations, thermodynamic calculations were performed using the PHREEQC program [8] and the ThermoChimic database [9]. These calculations were performed taking into account the measured pH, (8.7 ± 0.5) in both experiments, and the $E_{h(\text{vs SHE})}$, (-518 ± 50) mV for the experiment with the cladded pellet and (-418 ± 50) mV for the experiment with the fragments measured in solution at the end of both experiments.

As can be seen in figures 1 and 2, after a relatively high initial release the concentrations of ^{238}U decreases until approaching a virtually constant value at 1×10^{-8} M in both experiments. At the experimental pH and redox conditions, uranium is expected to be present as aqueous U(IV) species with low solubility controlled by a U(IV) solid in the long run. However, the relatively high initial release may be associated to the presence of oxidized layers on surfaces of the samples that release U(VI) to the solution.

According to the thermodynamic calculation U will be present in solution as $\text{U}(\text{OH})_4(\text{aq})$ as the predominant aqueous uranium species and $\text{UO}_2 \cdot x\text{H}_2\text{O}(\text{s})$ as the solubility controlling solid phase. The steady state reached in both experiments indicates that the uranium is not being released anymore from the SNF to the solution, this observation is related to the presence of H_2 in the system that will consume oxidants generated by water radiolysis, which could oxidize U(IV) on the SNF surface to more soluble U(VI) species. This effect has already been proposed by other authors [10-13].

In case of ^{237}Np , the concentration in both experiments was found stable at around 1×10^{-12} M. Similar to uranium, neptunium is a redox sensitive element. According to thermodynamic calculations, the predominant aqueous specie in solution is $\text{Np}(\text{OH})_4$ in equilibrium with $\text{NpO}_2 \cdot x\text{H}_2\text{O}(\text{s})$ as solid phase.

The concentration in solution of ^{239}Pu in both experiments does not exhibit an initial higher release. The concentration of plutonium in solution scattered in both experiments but apparently reached a steady state at about 1×10^{-11} M. Under these conditions, Pu is expected to be present in solution as Pu(III) with $\text{Pu}(\text{CO}_3)_3^{3-}$, $\text{Pu}(\text{CO}_3)_2^-$ and $\text{Pu}(\text{CO}_3)^+$ as the main aqueous species; the solid phase controlling the solubility is PuO_2 .

Finally, the concentration of ^{243}Am and ^{244}Cm in the experiment performed with a cladded SNF pellet scattered from 1×10^{-13} M to 1×10^{-11} M around an average value of 1×10^{-12} M. In case of the experiment performed with SNF fragments aqueous concentration of ^{243}Am and ^{244}Cm could not be detected, because their concentrations were under the detection limit of the ICP-MS. According to our thermodynamic calculations, Am and Cm is expected to be present in solution as $\text{Am}(\text{CO}_3)_2^-$, $\text{Am}(\text{CO}_3)^+$, $\text{Cm}(\text{CO}_3)_2^-$, $\text{Cm}(\text{CO}_3)^+$ in equilibria with their respective solid phases $\text{Am}_2\text{O}_3(\text{s})$ and $\text{Cm}_2\text{O}_3(\text{s})$.

Quantification and speciation of ^{14}C from irradiated metals

Introduction

The activation product ^{14}C is produced by neutron capture reactions during reactor operation from precursor elements (^{14}N , ^{17}O , and ^{13}C) present as impurities in metallic parts of nuclear fuel assemblies.

In safety analysis of deep geological repositories for spent nuclear fuel, ^{14}C must be considered due to its long half-life (~ 5730 years) and assumed mobility after release from the waste. Corrosion of the replaced steel components of fuel assemblies possibly releases ^{14}C bearing volatile and/or dissolved compounds. Organic ^{14}C bearing compounds reveal a high mobility either in the aqueous or in the gaseous phase whereas volatile/dissolved inorganic ^{14}C bearing compounds are affected by various retention processes in the near-field of a repository.

In this study, the inventory of ^{14}C present in irradiated stainless steel is determined. Furthermore, the



Fig. 5: Images of the irradiated stainless steel plenum spring.

chemical form of ^{14}C released from the steel is analyzed. Experimentally measured radionuclide contents are compared to theoretically predicted inventories of the irradiated steel, obtained by means of Monte Carlo N-Particle calculations (MCNP-X).

Stainless steel sample origin, irradiation characteristics, and subsample preparation

The studied stainless steel spring was sampled from the plenum of fuel rod segment N0204 of the fuel rod SBS1108. The characteristics of the irradiation of the fuel rod were described in the previous section.

Images of the 10.422 g heavy plenum stainless steel spring are given in figure 5. The plenum spring is made of X7CrNiAl17.7, and had a dose rate of ~ 1600 mSv/h in contact.

Subsamples for dissolution experiments were dry cut using an IsoMet[®] Low Speed Saw (11-1180, Buehler Ltd.) equipped with an IsoMet[®] diamond wafering blade (11-4254, Buehler Ltd.). Cutting was performed very slow (5 - 10 hours per sample) to prevent overheating of the material. Three subsamples with masses ranging from (47 ± 0.2) mg to (356 ± 0.2) mg were prepared by remote handling in a shielded box. Masses and dose rates were measured using an analytical balance and a dose rate meter. Dose rate of the subsamples was typically less than 230 mSv/h. Due to the high dose rate of the subsamples, also dissolution experiments had to be performed in a shielded box.

Dissolution of irradiated stainless steel subsamples

A stainless-steel specimen was placed in an autoclave equipped with a PTFE liner and a double-ended gas-collecting cylinder. The autoclave was flushed with argon for about 20 minutes. A mixture of 150 mL 24% H_2SO_4 + 3% HF was added through a tube using a syringe. After the addition, all valves in the lid of the autoclave were closed. The sample was digested within a day. However, to ensure complete digestion, sampling of the gaseous and aqueous phase was performed on the following day. Photos of the experimental set-up are shown in figure 6.

The evacuated gas-collecting cylinder was opened and the gas phase collected within two minutes. Finally, the autoclave was opened and the digestion liquor

was sampled. The gas-collecting cylinder was removed from the shielded box and the collected gas phase was analyzed by means of a multipurpose mass spectrometer with customized gas inlet systems (GAM 400, InProcess Instruments). Aliquots of the digestion liquor (after dilution due to dose rate) as well as the remaining gas phase in the gas collecting cylinder were also analyzed for ^{14}C in the extraction and analysis system installed in a glove box, as described in detail elsewhere [14]

Activation calculation for stainless steel radionuclide inventory prediction

The activation of the stainless-steel plenum spring was calculated by means of MCNP-X with its burn-up and activation module CINDER [15]. The nuclear data library used was the ENDF/B-VII database [16]. The simulation is based on a fuel subassembly of the PWR Gösgen core in which the fuel rod segment SBS1108-N0204 was inserted. Since the MCNP-X transport code evaluates the neutron flux of the subassembly, the input parameters include geometrical shape, material composition, and irradiation characteristics etc. of the subassembly. The obtained zone and energy dependent fluxes are forwarded to CINDER allowing for enhanced accuracy of the reaction rates evaluations upon which the activity of the relevant nuclides is determined. The properties of the plenum spring (mass, density, and dimensions) were accounted for in such a way it will include as much as possible all heterogeneity effects around the fuel rod segment. Thereby, the local neutron flux within the plenum could be simulated more accurately.

Since the exact composition of the stainless-steel spring is not available, nominal chemical composition data was used for simulation of the neutron flux and consequently for the activation calculation.

Results of experimental inventory analysis of irradiated stainless steel and chemical form of ^{14}C released from the studied material

Mean values of the experimentally determined ^{14}C inventory of the irradiated stainless steel plenum



Fig. 6: Autoclave for dissolution experiments, loaded with a steel specimen, inside a shielded box. The gas-collecting cylinder is not yet connected to the autoclave.

Tab. 1: Mean value of the experimentally determined inventory of ^{14}C in comparison with results from the activation calculation performed in this study.

	experimental [Bq/g]	calculated [Bq/g]	ratio
^{14}C	$2.7(\pm 0.3)\times 10^5$	$8.5(\pm 0.9)\times 10^4$	3.2

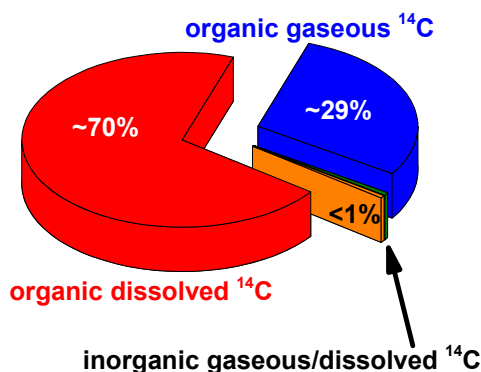


Fig. 7: Distribution of inorganic and organic ^{14}C bearing compounds in the gaseous and aqueous phase.

spring are summarized in Table 1. The experimentally determined ^{14}C inventory is further compared to theoretically predicted inventory obtained by MCNP calculations. Experimental and calculated results agree within a factor of about three. Given the limited knowledge of the nitrogen impurity in the irradiated steel and the great uncertainty of nitrogen contents in stainless steel in general (from 0.04 to 0.1 in weight % [17]), the experimental results obtained in the digestion experiments for ^{14}C is in good agreement with the calculated value. Experimental ^{14}C inventory in irradiated stainless steel, recently assessed by [17], exceeds the calculated value by a factor of four. It is noticeable that in both studies the experimentally determined inventory exceeds the calculated inventory by similar factors.

Moreover, about 99% of the ^{14}C is found as gaseous or dissolved organic ^{14}C bearing compounds after release from steel. These results are in accordance with results obtained on the chemical form of ^{14}C after release from irradiated Zircaloy-4 cladding [14]. The partitioning of ^{14}C bearing compounds in inorganic and organic fractions and their distribution in the gaseous and aqueous phase is provided in figure 7.

About $(70 \pm 10)\%$ of the ^{14}C inventory present in irradiated stainless steel is released as dissolved organic ^{14}C bearing compounds in the acidic digestion liquor. About $(29 \pm 10)\%$ of the ^{14}C inventory is released as gaseous ^{14}C bearing compounds during dissolution into the gas phase. Almost no inorganic ^{14}C bearing compounds ($< 1\%$) are found in all experiments neither in the gaseous nor in the aqueous phase.

References

- [1] Johnson, L., Ferry, C., Poinssot C., Lovera, P. *J. Nucl. Mater.*, 346, 56-65(2005).
- [2] Metz, V., Geckeis, H., González-Robles, E., Loida, A., Bube, C., Kienzler, B., *Radiochimica Acta.*, 100, 699-713 (2012).
- [3] Metz, V., González-Robles, E., Kienzler, B., KIT Scientific Reports, Karlsruhe KIT-SR 7676, 55-60 (2014).
- [4] González-Robles, E., Wegen, D. H., Metz, V., Herm, M., Papaioannou, D., Bohnert, E., Gretter, R., Müller, N., Nasyrow, R., der Weerd, W., Wiss, T., Kienzler, B. *J. Nucl. Mater.*, 479, 67-75 (2016).
- [5] González-Robles, E., Wegen, D. H., Bohnert, E., Papaioannou, D., Müller, N., Nasyrow, R., Kienzler, B., Metz, V. *Mat. Res. Soc. Symp. Proc.*, 1665, 283-289 (2014).
- [6] Wegen, D.H., Papaioannou, D., Gretter, R., Nasyrow, R., Rondinella, V.V., Glatz, J.-P. KIT-SR 7639, 193-199 (2013).
- [7] Loida, A., Gens, R., Metz, V., Lemmens, K., Cachoir, C., Mennecart, T., Kienzler, B. *Mat. Res. Soc. Symp. Proc.*, 1193, 597-604 (2009).
- [8] Parkhurst, D.L. and Appelo, C.A.J. U.S. Geological Survey Techniques and Methods, book 6, chap. A43, (2013).
- [9] Giffaut, E., Grivé, M., Blanc, P., Vieillard, P., Colàs, E., Gailhanou, H., Gaboreau, S., Marty, N., Madé, B., Duro, L. (2014). *Appl. Geochem.*, 4, 225-236 (2014).
- [10] Spahiu, K., Werme, L., Eklund, U.-B. *Radiochim. Acta*, 88, 507-511(2000).
- [11] Röllin, S., Spahiu, K., Eklund, U.-B. *J. Nucl. Mater.*, 297, 231-243(2001).
- [12] Loida, A., Metz, V., Kienzler, B., Geckeis, H. *J. Nucl. Mater.*, 346, 24-31(2005).
- [13] Fors, P., Carbol, P., Van Winckel, S., Spahiu, K. *J. Nucl. Mater.*, 394, 1-8 (2009).
- [14] Herm, M. PhD thesis. Karlsruhe Institute of Technology (KIT), Karlsruhe, 2015.
- [15] Pelowitz, D.B. LA-CP-11-00438 (2011).
- [16] Chadwick, M.B., Herman, M., Oblozinsky, P., Dunn, M.E., Danon, Y., Kahler, A.C., Smith, D.L., Pritychenko, B., Arbanas, G., Arcilla, R., Brewer, R., Brown, D.A., Capote, R., Carlson, A.D., Cho, Y.S., Derrien, H., Guber, K., Hale, G.M., Hobbitt, S., Holloway, S., Johnson, T.D., Kawano, T., Kiedrowski, B.C., Kim, H., Kuniyeda, S., Larson, N.M., Leal, L., Lestone, J.P., Little, R.C., McCutchan, E.A., MacFarlane, R.E., MacInnes, M., Mattoon, C.M., McKnight, R.D., Mughabghab, S.F., Nobre, G.P.A., Palmiotti, G., Palumbo, A., Pigni, M.T., Pronyaev, V.G., Sayer, R.O., Sonzogni, A.A., Summers, N.C., Talou, P., Thompson, I.J., Trkov, A., Vogt, R.L., van der Marck, S.C., Wallner, A., White, M.C., Wiarda, D., Young, P.G. Nucl. Data Sheets, 112, 2887-2996 (2011).

- [17] Schumann, D., Stowasser, T., Volmert, B., Günther-Leopold, I., Linder, H.P., Wieland, E. *Anal. Chem.*, 86, 5448-5454 (2014).

Acknowledgement

The research was partially funded by the European Union's Seventh Framework Program for research, technological development and demonstration under grant agreement no. 604479, the CAST project.